

# Numerical Analysis of Fluid Flow Characteristics inside Micro Channel

Sahu Jugal Kumar<sup>1</sup>, Ray Rashmi<sup>2\*</sup>

<sup>1,2</sup>ITER, Bhubaneswar, India

\*Corresponding author E-mail: [rashmiray@soa.ac.in](mailto:rashmiray@soa.ac.in)

## Abstract

In accordance to the advancement in the field of technology, modern society has privilege to have access to multifunctional devices. Indeed, the life has become surprisingly easier than preceding era, where as it brings its own consequence in terms several life-threatening diseases due to lack of physical activity. One of the most oozing out concern of the world is heart disease facilitated by cholesterol deposition in the arteries. In preceding years several researchers have put enormous effort to deepen understanding of this disease. Here in this study, computational fluid dynamics based finite element method commercial software COMSOL is used for numerical simulation of blood flow through the stenosed artery. The incompressible Navier Stokes equation is used for modeling blood flow in constricted channel. The blood is modeled as non-Newtonian fluid with the help of Carreau model. Various shape of constricted channel is considered to depict several biological occurrences of the blockage. Wide range of parameters such as blockage ratio ( $B = 10\text{-}50\%$ ), blood viscosity and blood velocity are evaluated to explore the phenomena of flow skewness and to explore the recirculation phenomena in the blood flow stream past partially blocked artery.

**Keywords:** Carreau model; Microchannel; Nanofluid; Slip flow; Tapered artery

## 1. Introduction

The modern lifestyle has a number of adverb patterns have negative effects on health physically, psychologically, and socially. One of these modern ways of living is the high intake of fast foods [1-3]. Not only fast food, but our polluted environment also affects the human heart which is a major problem nowadays. Normally most of the heart problems are caused due to the cholesterol deposit. Cholesterol and plaques can be the cause of heart disease. Plaques begin in artery walls and grow over years. The growth of cholesterol plaques slowly blocks blood flow in the arteries. Worse, a cholesterol plaque can suddenly rupture [4-5]. Reducing cholesterol and other risk factors can help prevent cholesterol plaques from forming. Occasionally, it can even reverse some plaque buildup. Our work is to analyze the fluid flow and heat transfer characteristics of blood inside blocked arteries [6-8].

## 2. Methodology

The Finite element analysis (FEA) is the simulation of any given physical phenomenon using the numerical technique called Finite element method (FEM). Finite element method is a numerical method for solving problems of engineering and mathematical physics. One of the Finite element method software COMSOL is used for numerical simulation. Before proceeding for application of the prepared model in COMSOL 4.3b, it is indispensable to access the accuracy and capability of the setup to solve different types of problem. Hence wide range testing has been done for different types of fluid flow and fluid structure interaction problem. The obtained results are compared with well-established

results obtained in literature. The cases for validation are chosen in such a way that all the cases have been widely investigated. All the validating results are represented in the subsequent discussions. Generally, COMSOL solvers take all the input parameter in dimensional form. To make the inputs in non-dimensional form, we have modeled the setup interns of reference scale. The detail modeling strategies will be described in the respective sections.

### 2.1 Flows over Stationary Cylinder in Infinite Domain

Formation of wake behind a sphere is a common phenomenon, when a moving fluid interacts with stationary body or vice versa. On the downstream side low pressure vortices are created and the object will tend to move towards the low-pressure zone. In this condition, vortices are generated and detached periodically from either side of the body. This phenomenon is widely available in nature also. Hence, at initial step we have chosen this problem to be solved by the setup prepared [7].

The domain is chosen in such way to ensure that the size must not affect the solution. The diameter ( $D$ ) of the cylinder is chosen to be 1unit. The length ( $L$ ) and height ( $H$ ) of the channel is set to  $27D$  and  $16D$  respectively. The position of the cylinder is fixed at  $7D$  from the inlet and  $8D$  from the bottom face as shown Fig.1. Appropriate boundary condition is imposed on all the boundaries for well implementation of problem. In Fig1 the left boundary is assigned with inlet, where the fluid is assumed to enter the domain at uniform velocity. Right boundary is assigned with outflow boundary condition. In such case, a zero-diffusion flux is assumed for all flow variables. Top and bottom boundary is identified as symmetry boundary condition, on which the velocity gradient in normal direction is assumed to be zero.

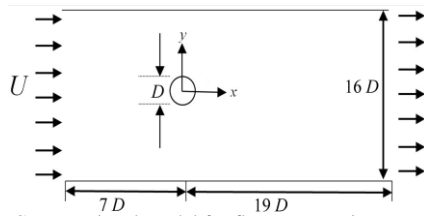


Fig 1: Computational model for flow over stationary cylinder

The fluid property is defined in such a way that  $Re$  can be regulated by changing only dynamic viscosity ( $\mu$ ) as we usually do in non-dimensional analysis. The computational domain is meshed by using 27986 number of triangular unstructured elements. The coefficient of drag and lift on the cylinder wall are calculated and compared with Dalal et al. [9]. The results obtained are in good agreement. Also the flow structures obtained possess well similarity with the previously obtained well established results.

Table 1: Comparison of simulated values of drag coefficient (CD) at different  $Re$  with Dalal et al.

$Re$	Dalal et al.*[9]	COMSOL Result	Percentage error
10	2.96	3	1.13
20	2.14	2.25	5.14
40	1.59	1.67	5.03
100	1.412	1.41	2.69

From the above discussion it is very clear that our simulation results possess good agreement with the reference results.

### 2.2. Flow over Stationary Cylinder Placed between Two Parallel Plates

Flow over isolated cylinder is widely studied with reasonably well accuracy. In extension to this, cylinder placed near a plane wall on either side or both sides is also abundant in real world. The fluid dynamic behavior of the flow pattern generated in this case has significant difference than that of the previous. In this portion the incompressible flow past a circular cylinder confined in a channel is studied and compared with Singha and Sinhamahapatra [10]. The computational model used for the simulations is as shown in the Fig.2.

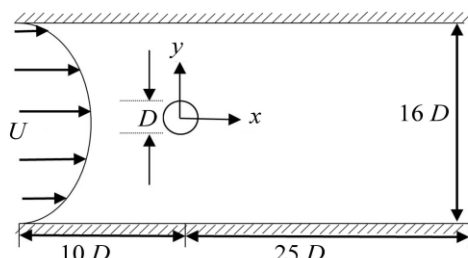


Fig.2: The schematic diagram of computational domain used for simulation of flow past circular cylinder placed inside a channel.

Due to the two-dimensional nature of the flow, there is no flow in  $z$  direction. Hence the solution will be governed by unsteady two dimensional Navier-Stokes equation and the boundary conditions are applied as follows. In Fig.2 the left boundary is assigned with inlet boundary condition, where velocity is defined by a fully developed parabolic velocity profile equation. The right boundary is identified as outflow boundary condition i.e. Neuman boundary condition. The top and bottom boundaries are defined as wall with no slip boundary condition. In addition to this on the surface of cylinder, as usual no slip boundary condition is applied. The authenticity of the setup is evaluated by comparing coefficient of drag (CD) with Singha and Sinhamahapatra [10] for various blockage ratio ( $\beta$ ) at two  $Re$ . The detail comparison is represented in tabular form in Table 2. The computational model used for

simulations is meshed by using 13876 number of triangular unstructured elements.

Table.2: Comparison of drag coefficient (CD) at different with Singha and Sinhamahapatra [10]

$Re$	$\beta$	Singha et al.[10]	COMSOL Result	Percentage error
45	4	1.83	1.7	7.10
	6	1.54	1.58	2.59
	8	1.44	1.39	3.47
100	4	1.40	1.33	5
	6	1.29	1.23	3
	8	1.26	1.23	2.38

### 2.3 Nanofluid Flow in a Long Microchannel with Slip Flow

The forced convection of Newtonian homogeneous nanofluid flow in a long microchannel is studied numerically under the influence of a magnetic field. The hot inlet nanofluid is cooled by the heat exchange with the cold microchannel walls. In this portion the incompressible flow through a microchannel with slip velocity is studied and compared with Karimipoura, D'Orazio&Shadloo [11]. The computational domain used for the simulation is shown in the fig 3.

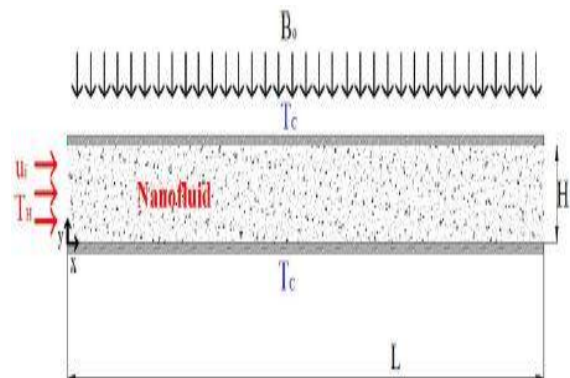


Fig.3 The schematic diagram of computational domain used for simulation of flow in a microchannel with slip velocity.

The solution will be governed by unsteady two dimensional Navier-Stokes equation and the boundary conditions are applied as follows. Here the temperature of the boundary is taken as constant. Slip velocity and temperature jump boundary conditions are simulated along the microchannel walls at different values of slip coefficient. The authenticity of the setup is evaluated by comparing Maximum Velocity for different values of Slip Coefficient ( $B$ ) with Karimipoura, D'Orazio&Shadloo [11]. The detail comparison is represented in tabular form in Table 3.

Table.3: Comparison of comparing maximum Velocity for different values of Slip Coefficient ( $B$ ) with Karimipoura, D'Orazio&Shadloo [11]

Slip Coefficient ( $B$ )	Maximum Velocity		Percentage error
	Karimipouret al.[11]	COMSOL Result	
0.01	0.05	0.05	0
0.05	0.23	0.227	1.3
0.1	0.37	0.37	0

Here is the Graphical comparison of the maximum Velocity for different values of Slip Coefficient ( $B$ ) are shown in the Fig. 4.

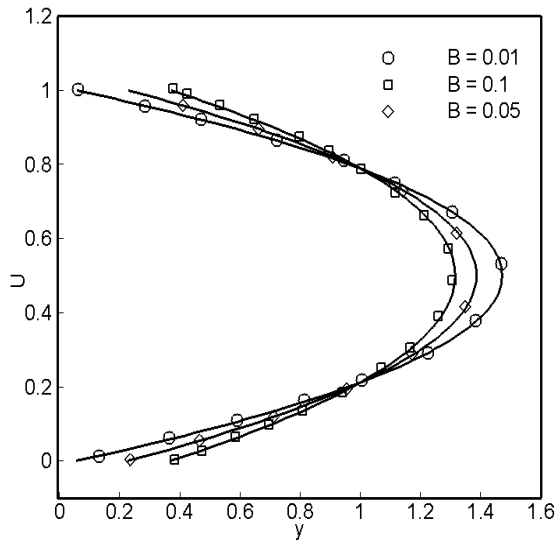


Fig.4: The graphical comparison of the maximum Velocity for different values of Slip Coefficient ( $B$ ).

After the validation the computational domain is modeled by using COMSOL for simulation. Observation of heat transfer and fluid flow characteristics in a micro channel with blockage ratio 50% is done.

### 3. Specification Of Problem

Steady state fluid is flowing through a circular micro channel (similar to artery of human heart) of constant cross section as shown in Fig.5. The diameter of the channel is  $100\mu\text{m}$  and the length of the channel is taken as  $1000\mu\text{m}$ .

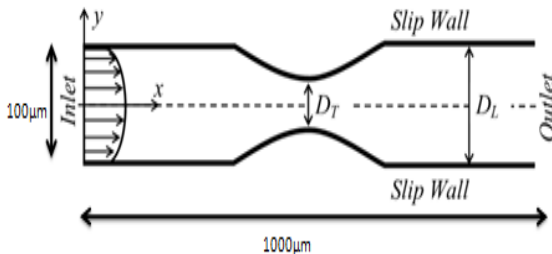


Fig5: Fluid flow through a Double stenosed artery

For calculation we considered a Carreau fluid model. Two-dimensional Navier-Stokes equations, continuity equation, and momentum equations are applied.

For modelling of blood viscosity, we used Carreau fluid model [12]

Carreau fluid model

$$\mu = \mu_{\infty} + (\mu_0 - \mu_{\infty}) [1 + (\lambda\dot{\gamma})^2]^{\frac{(n-1)}{2}}$$

Where

$$\mu_{\infty} = 0.0345 \text{ p} = 0.00345 \text{ pa.s}$$

$$\lambda = 313 \text{ s } 1 \text{p(poise)} = 0.1 \text{ pa.s}$$

$$n = 0.3568$$

$$\mu_0 = 0.56 \text{ p} = 0.056 \text{ pa.s}$$

$$\rho = 1060 \text{ kg/ m}^3$$

By taking a real human artery model the velocity and blood properties are considered and the computation processes are conducted.

### 3.1 Blood Flow inside Single Corrugated Artery

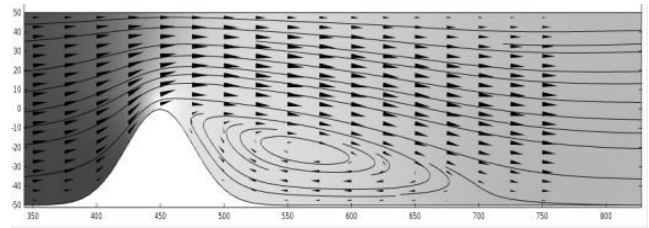


Fig 6: Fluid flow through a single tapered artery

This is the model for the blood flow inside a single corrugated artery with blockage ratio of 50%. For the second problem statement different cases are analysed to observe the flow characteristics like all the boundary conditions are remaining same with the previous problem. With different  $Re$  and different blockage ratios for  $Re$  100, the flow properties are also observed.

## 4. Result and Discussion

### 4.1 Analysis of Blood Flow inside Double Corrugated Artery

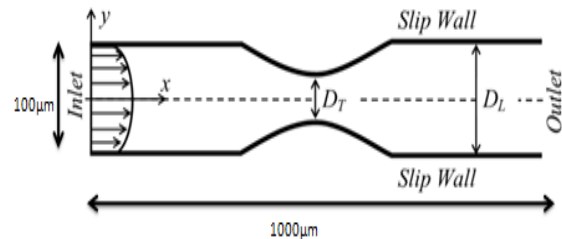
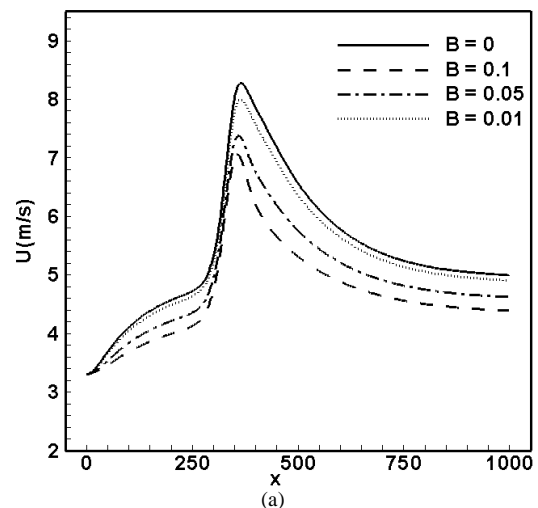


Fig 7: Fluid flow through a Double stenosed artery

To observe the effect of slip velocity we took different slip length  $B$  with respect to  $n=0.35$ . In COMSOL a horizontal line is considered to observe the velocity and pressure drop across the channel.

Table 4: Variation of  $u_{\text{max}}$  and Pressure Drop ( $p$ ) at throat for different slip length at  $n=0.35$

B	$u_{\text{max}}$ (m/s)	$p$ (pa)
0	8.27	-5700
0.1	7.06	-6550
0.05	7.38	-5300
0.01	8	-5150



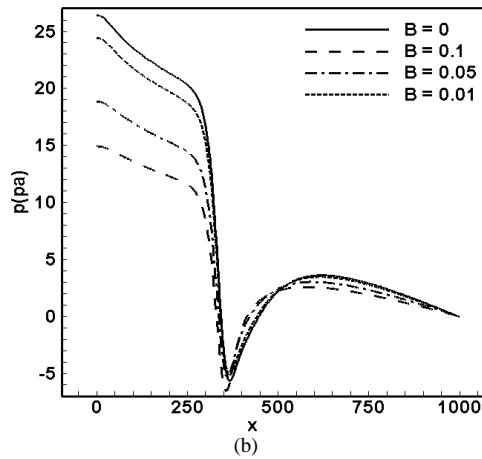


Fig 8: velocity  $u_{max}$ (a) and Pressure Drop  $p$  (b) plots for Different Slip velocity co-efficient (B) for  $n = 0.35$  across the channel.

We took another line at the throat to find out the change of pressure drop and velocity on the throat line for different slip velocity coefficient. The results are given below.

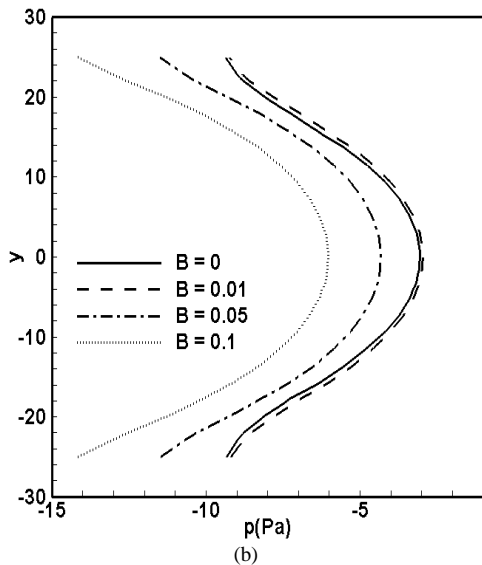
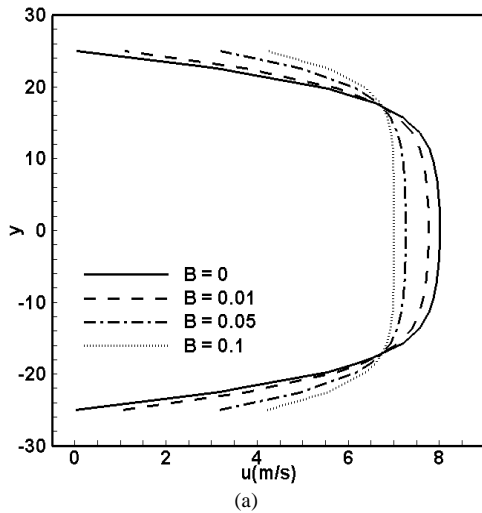


Fig 9: velocity  $u_{max}$ (a) and Pressure Drop  $p$  (b) plots for different Slip velocity coefficient(B) for  $n = 0.35$  On throat

To check the effect of  $n$  some models are created with constant  $B$  for  $n= 0.1, 0.2, 0.35, 0.5, 0.6, 0.7, 0.8, 0.9, 0.95$ . The maximum velocities and pressure drop for the  $n$  are given in the table.

Table 5(a) and (b): Variation of  $u_{max}$  and  $p$  along the channel for slip length (B) at different  $n$

n	B=0		B=0.1	
	$U_{max}$	P	$U_{max}$	P
0.1	8.28	-	7.06	-
		5700		6555
0.2	8.28	-	7.06	-
		5700		6555
0.35	8.27	-	7.06	-
		5700		6550
0.5	8.28	-	7.07	-
		5500		6523
0.6	8.29	-	7.08	-
		5060		6050
0.7	8.36	-	7.14	-
		3200		4695
0.8	8.6	0	7.36	-50
0.9	9.14	-440	7.75	-300
0.95	9.3	-	7.89	-750
		1000		

(a)

n	B=0.05		B=0.01	
	$U_{max}$	P	$U_{max}$	P
0.1	7.37	-5390	8	-
				5200
0.2	7.37	-5350	8	-
				5190
0.35	7.38	-5300	8	-
				5150
0.5	7.38	-5200	8	-
				5000
0.6	7.4	-4800	8.02	-
				4500
0.7	7.46	-3250	8.08	-
				2800
0.8	7.69	-50	8.32	-50
0.9	8.13	-350	8.8	-400
0.95	8.31	-930	9.02	-
				1000

(b)

The results are plotted on TECHPLOT and the effects on velocity and pressure are observed.

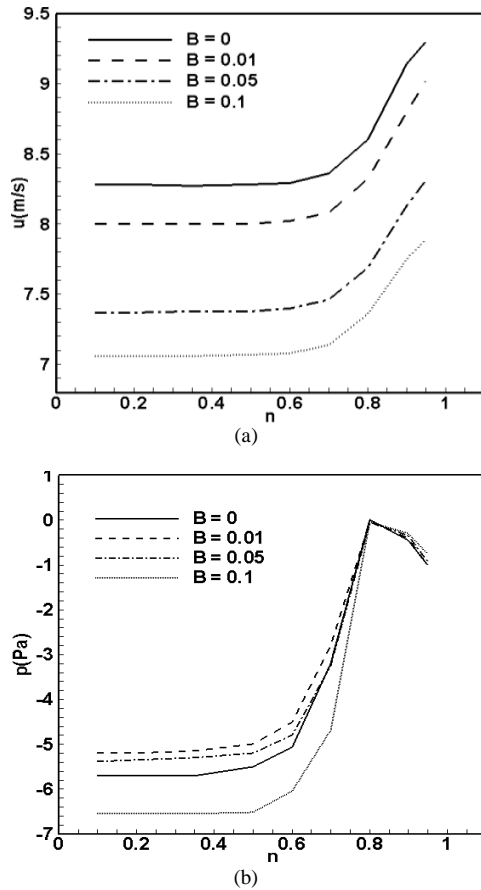


Fig 10: Variation of  $u_{max}$  (a) and Pressure Drop  $p$  (b) at different  $B$  with respect to  $n$  along the channel

To observe the effect and changes in velocity and pressure across the throat some more models are created and simulated. And the results are given in the figure 11.

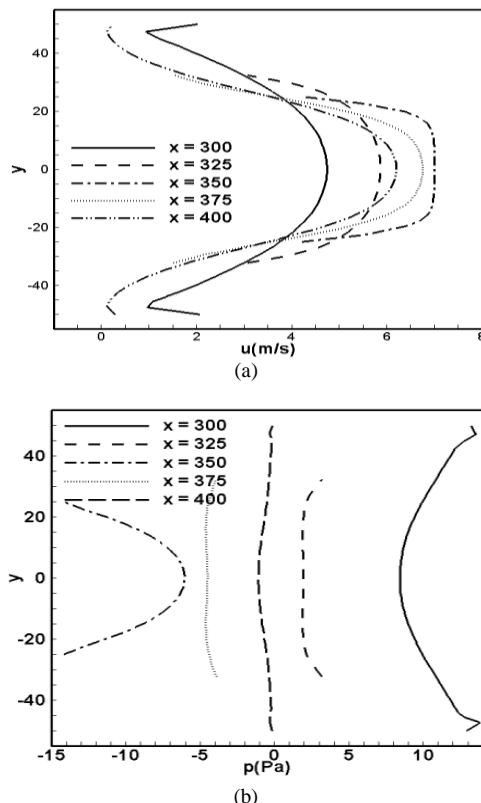


Fig 11: Variation of  $u_{max}$  (a) and  $P$ (b) across the throat region

### 4.2 Analysis of Blood Flow inside Single Corrugated Artery

After observing the fluid flow properties in a tapered artery with stenosis in both side, we simulated some models similar to a human artery with stenosis (from 10% to 50%) in one side. And then different  $Re$  are taken (from  $Re_{100}$  and  $Re_{500}$ ).

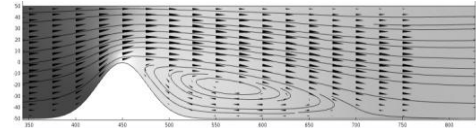


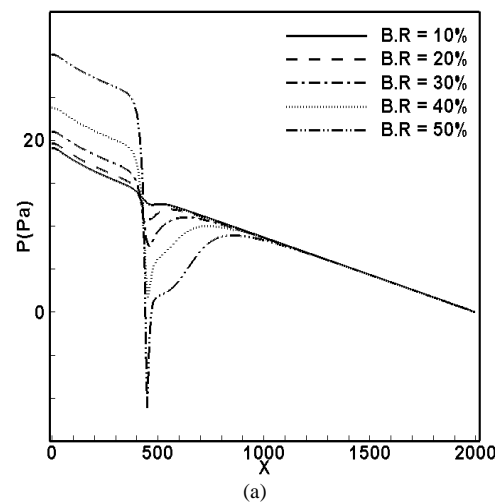
Fig 12: blood flow inside single corrugated artery

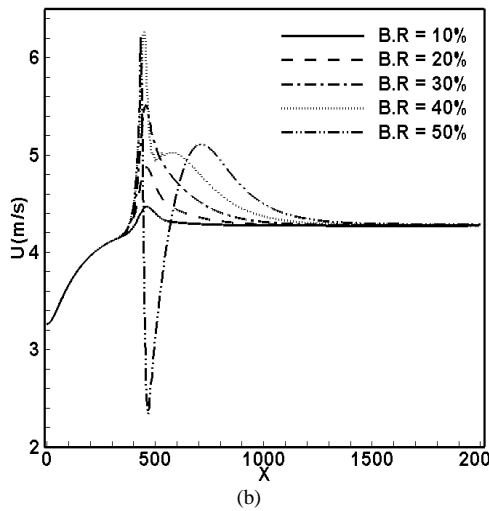
We found a circulation in flow after the blockage. Due to a lot of change in kinetic energy there is a circulation takes place. To observe the effect of slip velocity we took different slip length  $B$  with respect to  $n=0.35$ . In COMSOL a horizontal line (point1=(0,0) to point2=(0,2000)) is considered to observe the velocity and pressure drop across the channel along the microchannel. The maximum velocity and pressure drops are observed for different blockage ratios and different  $Re$ . By taking the values graphs are plotted.

Table 6: variation in pressure drop ( $P$ ) and flow velocity with blockage ratio

Blockage Ratio (B.R)	$u_{max}$ (m/s)	$p$ (Pa)
10%	4.4707	12513
20%	4.8754	10815
30%	5.5117	7714
40%	6.264	1724
50%	6.265	-11107

From the above table we can observe that the pressure decreases rapidly by increase in blockage ratio. There is a circulation from 30% to more. The flow velocity increases as the blockage ratio increases. From the table we can see that, at 40% to 50% blockage the velocity change became less. Due to increase in blockage ratio the cross-sectional area decreases. Therefore, the velocity of the flow increases rapidly. Increase in velocity a flow separation leads to the recirculation of blood creating a dead zone just after the throat.





**Fig13** Pressure Drop p (a) and velocity  $u_{max}$ (b) for Different Blockage Ratio (B.R.) along the channel

From the plots it is clearly observed as the B.R increases the pressure drops. The throat is at  $x=350$  but from the figure 13(a) it is clearly visible that the pressure drops just after the blockage and for B.R 50% the pressure drop is maximum. Figure 13(b) shows the change in velocity.

For 50% blockage as it can be observed that, the velocity increases at  $x=350$ (throat height is maximum), after that the velocity suddenly drops and the again increase and became steady. This creates the skewness in the flow. Due to increase in velocity the blood flows through artery rapidly leads to a flow separation and pressure drop. Pressure drop leads to dead zone, and a dead zone near a partially blocked artery can create a complete blockage.

After observing the changes in fluid properties, we have created different models to analyse the effect of Re in the flow. Here we can observe that for blockage ratio 50% there is sharp drop in velocity and then it increases to the maximum.

**Table 7:** Variation of  $u_{max}$  and p and vortex length along the channel for different Re

Re	$u_{max}$ (m/s)	p(pa)	Vl( $\mu$ m)
100	7.06	-6550	400
200	12	84651	650
300	18	168636	850
400	25	283688	1050
500	31	436656	1350

This table shows the change in pressure and velocity due to increase in Re. Due to increase in Re, the velocity and pressure drops increases and the vortex length became more. This leads to permanent blockage of the artery.

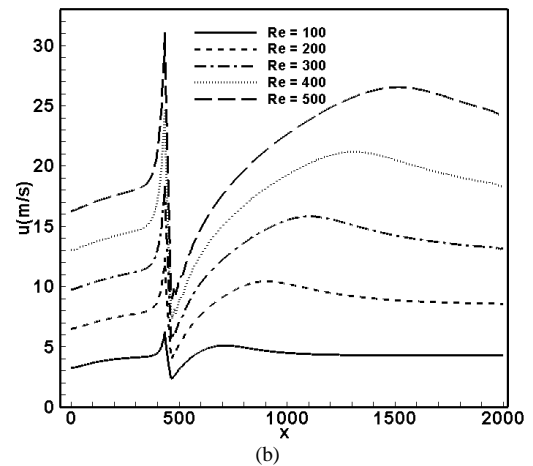
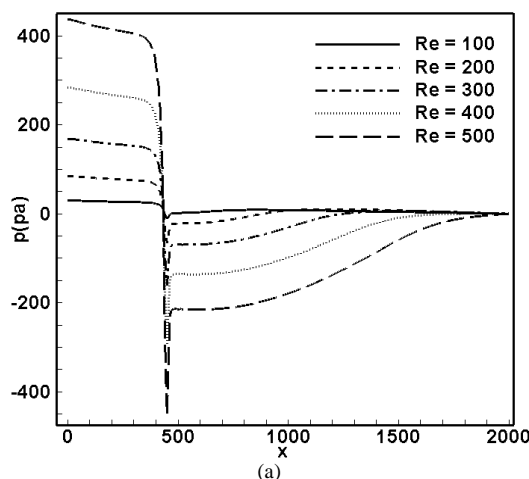


**Fig 14:** Pressure Drop p (a) and  $u_{max}$ (b) plots for Different Re for along the channel

Here as we can observe that, by increasing the Re the pressure drop also increases. velocity increases in the Re but there is a skewness in the flow. Table shows the increase in length of the vortex Vl with respect to Re.

**Table 8:** Variation of  $u_{max}$  and p and vortex length along the channel for different Re

Re	Image of the vortex created	Vortex length Vl
100		400
200		650
300		850
400		1050
500		1350

From the above table it can be observed that, as the Re increases the length of the vortex increases in a larger scale and the circulation became sharper. From the validation model we knew that due to blockage a flow separation takes place which helps in dropping the pressure that leads to cardiac diseases.

### 5. Conclusion

The numerical analysis of fluid flow properties through a tapered artery is done by using finite element based commercial software COMSOL Multiphysics. Different types of model are observed under different conditions with slip velocity. As we know in no slip over predict the actual velocity, so to study the real case we took slip boundary condition. Both single tapered and double tapered arteries are observed. For different slip velocity coefficient, varying blockage ratios and for different Re different models are analysed. From the analysis and by observing the results we found that

- With increase in the slip length coefficient the velocity increases and the pressure drop. Keeping slip velocity coefficient constant and varying the n, it is observed that, there is not much of change in velocity and pressure at low n. But for higher value of n the velocity increases rapidly and pressure decreases.
- In single corrugate ed artery, different amount of blockage are created (from 10% to 50%) to observe the changes in fluid properties. It is observed that as the blockage ratio increases the velocity increases and pressure decreases. Due to reduction in

cross sectional area of the microchannel the flow velocity increases rapidly creating a back pressure just after the throat region.

- The pressure drops suddenly at 40% to 50% blockage. Blockage creates a back pressure due to which flow separation occurs. The flow starts rotating after the blockage, which creates a dead zone. It is observed that blockage more than 40% is harmful to human artery.
- By changing the Re we observed the flow properties change. It is observed that at high Re, the recirculation length is more which means the pressure drop is more. Due to low pressure the deposition of the cholesterol increases which leads to complete blockage.

## References

- [1] Anagnostopoulos, P., & Minear, R. (2004). Blockage effect of oscillatory flow past a fixed cylinder. *Applied Ocean Research*, 26(3-4), 147-153.
- [2] Weilin Qu, Issam Mudawar. Experimental and numerical study of pressure drop and heat transfer in a single phase micro-channel heat sink. *International Journal of Heat and Mass Transfer* 45 (2002) 2549–2565
- [3] Barbara M. Johnston, Peter R. Johnston, Stuart Corney, David Kilpatrick. Non-newtonian blood flow in human right coronary arteries steady state simulations. *Journal of Biomechanics* 37 (2004) 709–720
- [4] Kh. S. Mekheimer, M. A. El Kot. The micropolar fluid model for blood flow through a tapered artery with a stenosis. *Acta Mech Sin* (2008) 24:637–644.
- [5] K. Hooman, A. Ejlali, Effects of viscous heating, fluid property variation, velocity slip, and temperature jump on convection through parallel plate and circular microchannels, *Int. Commun. Heat Mass Transf.* 37 (1) (2010) 34–38
- [6] H. Y. Wu and P. Cheng, An Experimental Study of Convective Heat Transfer in Silicon Microchannels with Different Surface Conditions, *Int. J. Heat and Mass Transfer*, ( 2003) vol. 46, pp. 2547–2556.
- [7] H. M. Badr, S. C. R. Dennis and P. J. S. Young., Steady and unsteady flow past a rotating circular cylinder at low Reynolds numbers. *Maxwell Pergamon Macmillan* (1989) 579-60
- [8] Anagnostopoulos, P., & Minear, R. (2004). Blockage effect of oscillatory flow past a fixed cylinder. *Applied Ocean Research*, 26(3-4), 147-153.
- [9] Amaresh Dalal , V. Eswaran & G. Biswas. A Finite-Volume Method for Navier-Stokes Equations on Unstructured Meshes .Taylor & Francis . 54: 238–259(2010)
- [10] Singha S., Sinhamahapatra K.P. Flow past a circular cylinder between parallel walls at low Reynolds numbers *Ocean Engineering* 37, 757–769-2010
- [11] Karimipoura et al (2017) The effects of different nano particles of Al<sub>2</sub>O<sub>3</sub> and Ag on the MHD nanofluid flow and heat transfer in a microchannel including slip velocity and temperature jump. *Physica E* . 146–153
- [12] Akbar & Nadeem, Carreau fluid model for blood flow through a tapered artery with a stenosis, *Ain Shams Engineering Journal* (2014) 5, 1307–1316